

A Generic Control Framework for Mobile Robots Edge Following

Mathieu Deremetz¹^a, Adrian Couvent¹^b, Roland Lenain¹^c, Benoit Thuilot²
and Christophe Cariou¹^d

¹Université Clermont Auvergne, Irstea, UR TSCF, Centre de Clermont-Ferrand,
9 avenue Blaise Pascal CS 20085, F-63178 Aubière, France

²Université Clermont Auvergne, CNRS, SIGMA Clermont, Institut Pascal, F-63000 Clermont-Ferrand, France

Keywords: Wheeled Robots, Field and Agriculture Robots, Edge Tracking.


Abstract: In this paper, the problem associated with accurate control for mobile robots following an edge is addressed thanks to a backstepping control. In particular, the control of the angular speed (control input) is investigated through the derivation of a new backstepping control by gathering derivatives regarding to time and to the curvilinear abscissa in a single framework. This new reference then allows both time and distance convergence of the robot states towards a trajectory computed with points given by a Lidar only. This permits to address the control of different kinds of robots (skid-steering, car like, four-wheel-steering) in a common framework and to consider independently the speed regulation, the lateral and the longitudinal controls. The control proposed here allows an accurate and reactive path tracking even if the environment is complex and narrow. The efficiency of the approach is investigated through full scale experiments in various conditions.


1 INTRODUCTION


Mobile robotics has raised as a promising solution to help people in everyday life and has been the subject of a lot of significant advances. The progress achieved on autonomous cars (Marmoulin and Slade, 2016) is one of the best examples, since first commercial solutions are about to be marketed. Human transportation is not the sole application area which may benefit from autonomous mobile robots and numerous social needs may be addressed thanks to this topic (Bergerman et al., 2016). This is particularly the case in environment and agriculture areas, where painful and dangerous works have to be achieved. As a result, the use of robots able to act autonomously to pull an implement or to carry out heavy loads may permit, among others, the reduction of the hardness of work or the limitation of the operator exposition to risks (Blackmore, 2016).


In this context, the autonomous motion task often consists in trajectory following, which has been deeply studied in the literature (Samson et al., 2016).

In open area, this can be easily achieved using a GPS sensors, offering permanently an absolute localization for the robot navigation (Cariou et al., 2010). Nevertheless, this sensor appears to be expensive and not always applicable, especially in vineyard or orchard applications. The height of the vegetation in these contexts may indeed lead to a bad reception of satellite signals. Moreover, since agricultural tasks have to be done with respect to crops, the regulation of the robot motion with respect to vegetation must be favoured. As a result, alternative approaches have been proposed, often based on artificial vision such as considered in (Cherubini and Chaumette, 2013), in (Tourrette et al., 2017), or in (Astrand and Baerveldt, 2005) for agricultural applications, or based on a Lidar, such as achieved in (Bayar et al., 2015). As soon as a local positioning is available, different control laws can then be applied (such as derived in (D'Andréa-Novell et al., 1995), or (Lenain et al., 2017)). Nevertheless, such approaches do not explicitly compute the angular orientation and are therefore not suitable when moving autonomously in narrow spaces, such as encountered for instance in vineyard, or when achieving harsh manoeuvres. Another approach introduced in (Deremetz et al., 2017) allows to control the absolute orientation of the robot with respect to the global

^a  <https://orcid.org/0000-0002-1239-0320>

^b  <https://orcid.org/0000-0002-3453-1358>

^c  <https://orcid.org/0000-0003-0348-8673>

^d  <https://orcid.org/0000-0002-7343-7452>

frame, but this latter is not available in the considered applications.

In this paper, an alternative approach of the trajectory tracking to follow an edge is proposed. It is based on a backstepping control, allowing to consider independently longitudinal and lateral controls and separate the position and the orientation servoing of the robot. This permits to improve the control of the robot orientation to improve manoeuvrability and avoid the collision with the structure to be followed. This control is generic and developed for several kinds of robots: skid-steering, car-like mobile, or four-wheel steering robots. In the latter case, the backstepping approach is enhanced in order to regulate the actual orientation of the robot in order to optimize the work of an on-boarded implement (which is important for agricultural tasks, such as spraying) as well as the manoeuvrability.

This paper is decomposed as follows. First, the kinematic model of a mobile robot with respect to an edge is recalled. Based on this generic modelling, the proposed backstepping control approach is detailed. Then additive features to improve manoeuvrability and safety are presented. Finally, the efficiency of the proposed control architecture is investigated through full scale experiments in various conditions, using several kinds of robots.

2 MODELLING

2.1 Assumptions and Notations

In this paper, the objective is to follow a structure, using an edge detector, thanks to a mobile robot. For that purpose, a control strategy based on the trajectory tracking point of view may be considered, as classically investigated in (Samson et al., 2016). In this point of view, a four-wheel-steering robot can be described as a bicycle such as depicted in Fig 1. The robot is reduced to two wheels, one for the front axle with a steering angle denoted as δ^F , and one for the rear axle, with an angle denoted δ^R .

The position of the robot is defined with respect to the detected structure Γ to be followed (considered as a trajectory), with a lateral error y , also called tracking error, and a curvilinear abscissa s (i.e. the distance achieved along the trajectory). Let us denote by $\tilde{\theta}$, the difference between the orientation of the robot and the direction of the tangent to Γ at the curvilinear abscissa s . The curvature of the trajectory to be followed at the curvilinear abscissa s is denoted by $c(s)$. With these notations the objective of the structure following strategy is to ensure the convergence

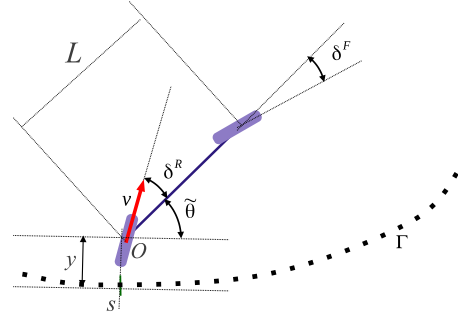


Figure 1: Modelling of the mobile robot w.r.t. the detected structure Γ .

of the lateral deviation y to some desired set point y_d , at a desired speed v_d . As it will be pointed out in the following, even if a four-wheel-steering robot is presented in this section, the proposed control strategy is also derived for a skid-steering robot or a car-like mobile robot (with only an inactive rear steering $\delta^R = 0$). The state vector associated to this framework may be defined as follows:

$$X = \begin{bmatrix} s \\ y \\ \tilde{\theta} \end{bmatrix}. \quad (1)$$

2.2 Motion Equations

Based on the notations introduced previously and according to (Samson et al., 2016), one can obtain the derivative of the state vector X with respect to time, which constitutes the evolution model for the path tracking problem.

$$\dot{X} = \begin{bmatrix} \dot{s} = \frac{v \cos(\tilde{\theta} + \delta^R)}{1 - yc(s)} \\ \dot{y} = v \sin(\tilde{\theta} + \delta^R) \\ \dot{\tilde{\theta}} = u_\theta - \frac{c(s)v \cos(\tilde{\theta} + \delta^R)}{1 - yc(s)} \end{bmatrix}. \quad (2)$$

The variable u_θ denotes the yaw rate of the robot, which is directly a control variable for a skid steering robot. For a four-wheel-steering robot, this variable depends on the values of the steering angles, which are the actual control variables. The relation between u_θ and these steering angles can be defined by the following relationship:

$$u_\theta = v \cos(\delta^R) \frac{\tan(\delta^F) - \tan(\delta^R)}{L}, \quad (3)$$

with L denoting the robot wheelbase. For a car-like mobile robot, the model (2)-(3) still stands by imposing a null rear steering angle ($\delta^R = 0$).

In this paper, another objective is to follow a structure relying on the travelled distance of the robot (that is to say independently from the robot's speed). As a result, the model (2) can be rewritten according to derivatives w.r.t. the curvilinear abscissa s instead of w.r.t. time. Let us define by $X' = \frac{dX}{ds}$, the derivatives of the variable X w.r.t. s . From (2) it can be expressed as:

$$X' = \begin{bmatrix} s' = 1 \\ y' = (1 - yc(s)) \tan(\tilde{\theta} + \delta^R) \\ \tilde{\theta}' = u_\theta \frac{1 - yc(s)}{v \cos(\tilde{\theta} + \delta^R)} - c(s) \end{bmatrix}. \quad (4)$$

The expression (4) exists for the last equation (yaw motion) if the longitudinal velocity v is not null. This assumption is not a limitation in the following since the synthesis of the control avoids this singularity.

3 PROPOSED CONTROL ARCHITECTURE

The control strategy proposed in this paper is based on a backstepping approach, which is summarized in Fig. 2. Using this principle, this control scheme can be adapted to several kinds of mobile robots using the same paradigm. Thanks to a detection algorithm, a reference trajectory is obtained and the state vector X may be known. In particular, the lateral deviation is measured and can be compared to the desired one y_d . The resulting error between these two values is then used to compute a desired orientation, allowing the robot to reach the desired lateral deviation under a desired distance. Thus, this orientation is used as a set point to compute a control law for the angular speed. For a skid-steering robot, this is directly the control imposed to the robot. For a four-wheel-steering robot, this permits to deduce the front steering angle.

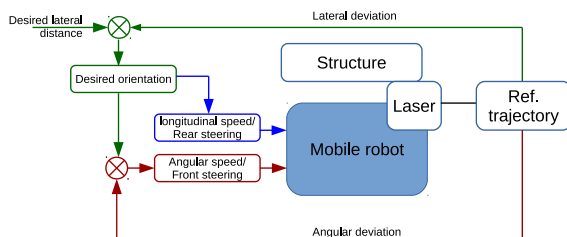


Figure 2: Synopsis of the proposed control architecture.

The desired orientation also permits to regulate the speed of the robot and the rear steering angle for a 4 wheel driven (4WD) robot:

- For a skid-steered robot, since the robot can turn on itself, the velocity is controlled independently

from the yaw rate, in order to improve the tracking accuracy and avoid collision.

- For a four-wheel-steering robot, the yaw rate can not be controlled regardless of the longitudinal velocity. Nevertheless, the rear steering angle can be actuated to improve the convergence of the robot or to control the actual orientation of the robot w.r.t. to the structure to be followed, impacting the convergence of the lateral error.

These different steps are detailed hereafter.

3.1 Computation of the Target Value of the Angular Deviation

From a control point of view, the objective of the structure following is to ensure the convergence of the lateral deviation y to some desired set point y_d , supposed to be constant $\dot{y}_d = 0$. Let us consider the error $e_y = y - y_d$, to be regulated to zero after a settling distance. Using the second equation of the model (4), one can write the derivative of this error with respect to the curvilinear abscissa:

$$e_y' = \alpha \tan(\tilde{\theta}_2), \quad (5)$$

with $\alpha = (1 - yc(s))$ and $\tilde{\theta}_2 = \tilde{\theta} + \delta^R$. Let us consider $\tan \tilde{\theta}_2$ as an intermediate control variable. One can note that if we impose for this variable the expression (6)

$$\tan \tilde{\theta}_d = \left(\frac{k_y e_y}{\alpha} \right), \quad (6)$$

the dynamic of the error (5) becomes:

$$e_y' = k_y e_y, \quad (7)$$

where k_y is a negative scalar that specifies the settling distance for the convergence of the lateral deviation of the robot to the desired lateral deviation y_d .

The virtual control value (6) of $\tilde{\theta}_d$ then constitutes a set point to be reached by θ_2 (reduced to the actual orientation $\tilde{\theta}$ in the case of skid-steering or car-like robots). For that purpose, let us consider the error defined as:

$$e_{\tilde{\theta}} = \tan \tilde{\theta}_2 - \tan \tilde{\theta}_d, \quad (8)$$

representative of the orientation error of the robot with respect to the desired orientation. The design of control laws ensuring the convergence of this error depends on the considered robot and is addressed in the two next sections.

3.2 Control Law Design for Skid-steering Robots

Since a skid-steering robot can turn on itself, the orientation of the robot may be regulated without taking

the longitudinal speed into account. As a result, one can consider the time derivative of the error (8) derived from the model (2), with $\delta^R = 0$:

$$\dot{e}_{\tilde{\theta}} = \frac{1}{\cos^2 \tilde{\theta}} \left(u_{\theta} - \frac{c(s)v \cos \tilde{\theta}}{\alpha} \right). \quad (9)$$

This expression is obtained by considering that the time derivative of the desired orientation may be neglected with respect to the reactivity of the angular speed regulation (i.e. $\dot{\tilde{\theta}}_d \approx 0$).

The convergence of the error $e_{\tilde{\theta}}$ to zero may be obtained by considering for the controlled angular speed of the robot, the control law (10) such that:

$$u_{\theta} = k_{\tilde{\theta}} e_{\tilde{\theta}} \cos^2 \tilde{\theta} + \frac{c(s)v \cos \tilde{\theta}}{\alpha}. \quad (10)$$

This expression indeed imposes the condition (11) for the derivative of the angular error, where $k_{\tilde{\theta}}$ is a negative scalar that specifies the settling time of error dynamics.

$$\dot{e}_{\tilde{\theta}} = k_{\tilde{\theta}} e_{\tilde{\theta}}. \quad (11)$$

In this control, the assumption $\dot{\tilde{\theta}}_d = 0$, may be ensured by choosing $|k_{\tilde{\theta}}| \gg |k_y \dot{s}|$ ensuring that the orientation of the robot reaches the desired orientation fast enough.

The global stability of this two-steps backstepping control law may indeed be checked by considering the Lyapunov function candidate:

$$V = \frac{1}{2} \frac{k_{\tilde{\theta}} k_y}{\alpha^2 \dot{s}} e_y^2 + \frac{1}{2} \tan^2 \tilde{\theta}. \quad (12)$$

When considering that curvilinear velocity is strictly positive, and slow varying (as well as α), its time derivative can be expressed as:

$$\dot{V} = \frac{k_{\tilde{\theta}} k_y}{\alpha^2 \dot{s}} \dot{e}_y e_y + \frac{\dot{\tilde{\theta}}}{\cos^2 \tilde{\theta}} \tan \tilde{\theta}. \quad (13)$$

Considering that $\dot{e}_y = e'_y \dot{s}$, and expressions (5) for e'_y and (2) for $\dot{\tilde{\theta}}$, this derivative becomes.

$$\dot{V} = \frac{k_{\tilde{\theta}} k_y}{\alpha} \tan \tilde{\theta} e_y + \frac{u_{\theta} - \frac{c(s)v \cos \tilde{\theta}}{\alpha}}{\cos^2 \tilde{\theta}} \tan \tilde{\theta}. \quad (14)$$

Finally by introducing the control law (10) in (14) leads to the following expression for the derivative of the function V :

$$\dot{V} = k_{\tilde{\theta}} \tan^2 \tilde{\theta}. \quad (15)$$

which is negative and null if and only if $\tilde{\theta} = 0$.

Based on the fact that the function V defined by (12) is Lyapunov, one can deduce that the robot controlled using (10) is exponentially stable and ensures the convergence of e_y to zero (i.e. the robot converge to its desired set point). The definition of the function V exists providing that $\dot{s} > 0$ (i.e. the robot

goes ahead along the trajectory). When the robot stops, it can of course not converge to the desired set points. Nevertheless, the control law (10) can still be applied and the robot can turn on itself to reach the condition (6), and be oriented to reach the trajectory after a desired distance.

3.3 Control Law Design for the Front Steering Axle of Car-like or 4WD Robots

Since these two kinds of robots cannot turn when their longitudinal speed is null, the derivative of $e_{\tilde{\theta}}$ is derived this time from model (4) expressed with respect to the curvilinear abscissa. Relying on expression (3) and model (4), one can derive:

$$e'_{\tilde{\theta}} = \cos(\delta^R) \alpha \frac{\tan(\delta^F) - \tan(\delta^R)}{L \cos^3(\tilde{\theta}_2)} - \frac{c(s)}{\cos^2(\tilde{\theta}_2)}. \quad (16)$$

Once more, this expression is obtained by considering that $\tilde{\theta}_d$ is slow-varying w.r.t. the achieved distance ($\dot{\tilde{\theta}}'_d \approx 0$) compared to the yaw dynamics imposed to the robot. The convergence of this error to zero may then be imposed considering the control law (17) for the front steering angle:

$$\delta^F = \arctan \left(\tan(\delta^R) + \frac{L \cos^3(\tilde{\theta}_2)}{\alpha \cos \delta^R} \left(k_{\tilde{\theta}} e_{\tilde{\theta}} + \frac{c(s)}{\cos^2(\tilde{\theta}_2)} \right) \right). \quad (17)$$

Since control law (17) indeed leads to the following expression for the error dynamics:

$$e'_{\tilde{\theta}} = k_{\tilde{\theta}} e_{\tilde{\theta}}, \quad (18)$$

where $k_{\tilde{\theta}}$ is a negative scalar that specifies the settling distance of the convergence of $e_{\tilde{\theta}}$ to zero. In order for this settling distance to be shorter than the settling distance imposed on lateral error e_y , the condition $-k_{\tilde{\theta}} \gg |k_y|$ has to be satisfied

The global stability of this two-steps backstepping control can be established by straightforwardly deriving twice e_y w.r.t. the curvilinear distance and then injecting control law (17). One can indeed obtain:

$$e''_y = k_{\tilde{\theta}} e'_y - k_{\tilde{\theta}} k_y e_y. \quad (19)$$

This condition ensures the convergence of e_y to zero as soon as $k_{\tilde{\theta}}$ and k_y are negative.

If the robot is a car-like robot, then the expression (17) has to be directly applied with $\delta^R = 0$. For a four-wheel-steering robot, this control law may be computed providing that δ^R is known, which is normally ensured, since this variable is also controlled. An expression for this last control variable is detailed in the following section.

3.4 Control Law Design for the Rear Steering Axle of 4WD Robots

In the previous section, an expression for the front steering angle has been defined in order to impose that $\tilde{\theta}_2$ converges to some desired $\tilde{\theta}_d$. Nevertheless, the actual orientation of the robot stays uncontrolled and clearly relies on the rear steering angle. In steady state phases, since $e_{\tilde{\theta}}$ converges to zero, one indeed has:

$$\tilde{\theta} \rightarrow \tilde{\theta}_d - \delta^R . \quad (20)$$

To go further, one can then control the rear steering angle to regulate the actual robot orientation to some desired orientation $\tilde{\theta}_r$. For that purpose, let us define the error $e_r = \tan \tilde{\theta} - \tan \tilde{\theta}_r$. By properly tuning the gain of the forthcoming control law, the derivative w.r.t. s of the rear steering angle δ^R can be neglected. The derivative w.r.t. s of the error e_r can then be written as:

$$\begin{aligned} e_r' &= e_{\tilde{\theta}}' \\ e_r' &= k_{\tilde{\theta}} (\tan(\tilde{\theta} + \delta^R) - \tan \tilde{\theta}_d) . \end{aligned} \quad (21)$$

In view of this expression, the control law (22) can be defined for the rear steering angle.

$$\delta^R = \arctan \left(\frac{k_r e_r}{k_{\tilde{\theta}}} + \tan \tilde{\theta}_d \right) - \tilde{\theta} . \quad (22)$$

This control law indeed provides the error dynamics defined by the following differential equation:

$$e_r' = k_r e_r . \quad (23)$$

This ensures, providing that k_r is a negative scalar, that the angular deviation $\tilde{\theta}$ converges to the desired one $\tilde{\theta}_r$. This latter desired orientation may be defined at the user convenience. For instance one can set $\tilde{\theta}_r = 0$, to ensure that the robot is parallel to the structure, or $\tilde{\theta}_r = \tilde{\theta}_d$ to increase the manoeuvrability. In practice, it would be best to define $\tilde{\theta}_r$ as a function such that:

$$\tilde{\theta}_r = \begin{cases} 0 & \text{if } |\tilde{\theta}_d| < \tilde{\theta}_{th} , \\ \tilde{\theta}_d & \text{if } |\tilde{\theta}_d| > \tilde{\theta}_{th} , \end{cases} \quad (24)$$

where $\tilde{\theta}_{th}$ is a positive angle corresponding to the threshold where the robot behaviour changes (i.e. parallel to the structure or manoeuvrability increase). With this choice, if the robot is far from the desired distance, the rear steering angle helps the robot to converge to the set point, and if the robot is close to the desired position, the rear steering angle ensures that the robot is parallel to the structure. This is important when considering agricultural tasks, such as spraying, since the on-boarded implement must have a defined orientation. A commutation function may be used instead of the switch proposed by (24). A threshold of 15° is settled in this paper.

4 VELOCITY CONTROL AND COLLISION AVOIDANCE

In order to avoid collisions with the structure, a limitation of the desired orientation $\tilde{\theta}_d$ is introduced, depending on the robot size (track and wheelbase). It is here possible since the first step of the proposed back-stepping control design consists precisely in defining a desired orientation. Finally, since skid-steering robots are able to turn on themselves, a dedicated speed regulation law is proposed in order to enable a structure following including very small radii of curvature.

4.1 Limitation of the Robot Orientation

In Fig. 3, one can observe that when regulating a desired lateral distance, the front of the robot may touch the structure when this latter proposes important curvatures.

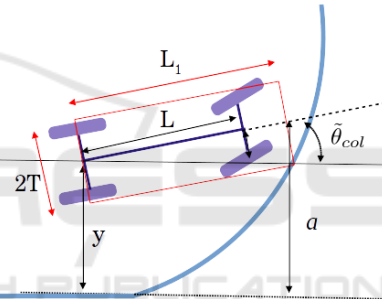


Figure 3: Case of collision while the robot is well regulated.

In such a configuration, the robot must overstep the nominal regulation laws and turn in order to avoid collisions. It is possible to compute the maximal admissible orientation of the robot to avoid the collision. This angle, denoted $\tilde{\theta}_{col}$, may be geometrically defined by:

$$y = a + T + L_1 \sin \tilde{\theta}_{col} , \quad (25)$$

with T the half-track of the robot and a the distance between the tangent at the trajectory and the impact point. If we consider that the trajectory is locally circular (such as suggested in Fig. 3), with a radius of $\frac{1}{c(s)}$, this distance a may be approximated by the following expression:

$$a = \frac{1 - \cos \gamma}{c(s)} , \quad (26)$$

with $\gamma = \arctan(L_1 c(s))$. The expression (25) exists under the condition $|\frac{y - V - a}{L_1}| < 1$, which means that the front of the robot stays on the good side of the structure, which is assumed to be the case in practice.

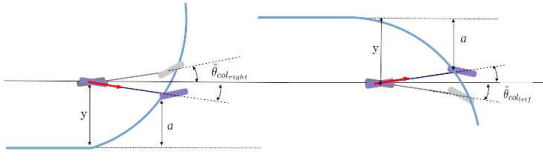


Figure 4: Case of collision on the right and the left.

Since the structure to be followed can be located on the right or on the left of the robot, $\tilde{\theta}_{col}$ has two possible values denoted $\tilde{\theta}_{col_{right}}$ and $\tilde{\theta}_{col_{left}}$, depending on the side where the structure is, as depicted in Fig. 4. As soon as these two limits are known, an advantage of the proposed backstepping approach lies in the fact that the desired orientation of the robot $\tilde{\theta}_d$, computed by the control law (6) can be bounded. In the following, the limits are computed in real time and the targeted orientation is defined such as:

$$\tilde{\theta} = \begin{cases} \xi & \text{if } \tilde{\theta}_{col_{right}} < \xi < \tilde{\theta}_{col_{left}}, \\ \tilde{\theta}_{col_{left}} & \text{if } \xi > \tilde{\theta}_{col_{left}}, \\ \tilde{\theta}_{col_{right}} & \text{if } \xi < \tilde{\theta}_{col_{right}}, \end{cases} \quad (27)$$

with $\xi = \arctan\left(\frac{k_y e_y}{\alpha}\right) - \delta^R$, such as defined by (6).

4.2 Limitation of the Robot Speed

In order to ensure an accurate edge tracking, it is relevant to take the actuator settling time into account. Indeed, the major consequences of this parameter are overshoots on the tracking error. To limit this phenomenon, it has been chosen to link the linear speed of the robot with its angular deviation with respect to the edge (i.e. $v = f(\tilde{\theta} - \tilde{\theta}_d) = f(e_{\tilde{\theta}})$). A profile, such as the one illustrated in Fig. 5 can be considered. This permits to adjust the linear speed of the robot when a tricky and narrow edge following appears.

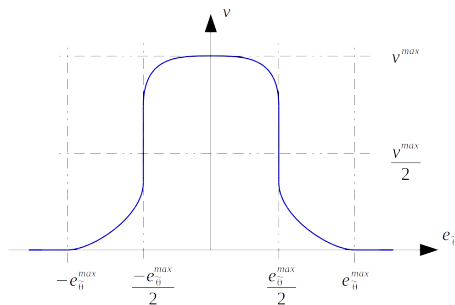


Figure 5: Dependency between the linear speed and the robot angular deviation.

Indeed, this profile is defined thanks to two parameters: the maximum linear speed of the robot v_{max} and a threshold in the orientation error $e_{\tilde{\theta}}$ chosen in

advance. As long as the absolute value of the error is lower than a threshold, the linear speed of the robot is positive. It decreases when the orientation error $e_{\tilde{\theta}}$ approaches the threshold angle and is null beyond. This is applied on a skid-steering robot, since it can turn on itself, and then resume its motion to ensure a relevant structure following.

5 EXPERIMENTAL RESULTS

5.1 Experimental Testbed

The proposed control framework has been tested on two robots in two different conditions, depicted in Fig. 6:

- a skid-steering mobile robot, moving in indoor conditions, and following several kinds of structure (box, wall, shelves), such as depicted in Fig. 6(a). It is a 25kg electric robot with a wheel-base of 0.6m. The Lidar is settled at 0.8m from the rear wheel;
- a four-wheel-steering mobile robot moving in off-road conditions, following a row of trees (see Fig. 6(b)). This is a 520kg robot with a 1.2m-wheelbase. The Lidar is situated at 1.8m from the middle of the rear axle.

Both of the robot are equipped with a Sick-LMS laser. The structures to be followed, quite different, are depicted by red lines in Fig. 6, reflecting some harsh curvature in indoor conditions and an almost straight line structure in outdoor conditions. The running direction is depicted by the pink arrow.

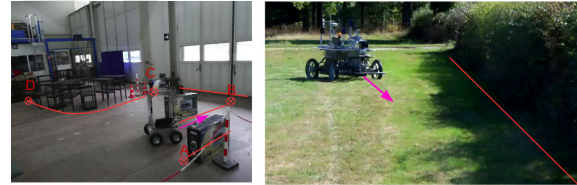


Figure 6: Robots during the experiments: (a) indoor skid-steering mobile robot (b) outdoor four-wheel-steering mobile robot.

The structures are detected relying on the algorithm described in Figure 7. It permits to obtain a relevant and smooth trajectory in both indoor and outdoor environments.

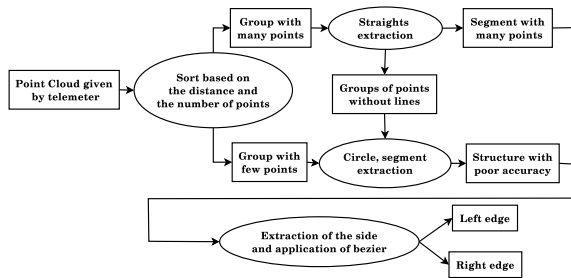


Figure 7: Algorithm to estimate surrounding structures.

5.2 Skid-steering Robot in Indoor Conditions

The first experiment proposed in this paper consists in an indoor structure following by the skid-steering mobile robot shown in Fig. 6(a). During this test, the robot follows a box on the right and then a box on the left (from A to B), it then follows a large door (from B to C), and shelf legs arranged in circle (from C to D). Fig. 8 shows a snapshot of the structure detection and the trajectory generated when the robot is following the structure from C to D.

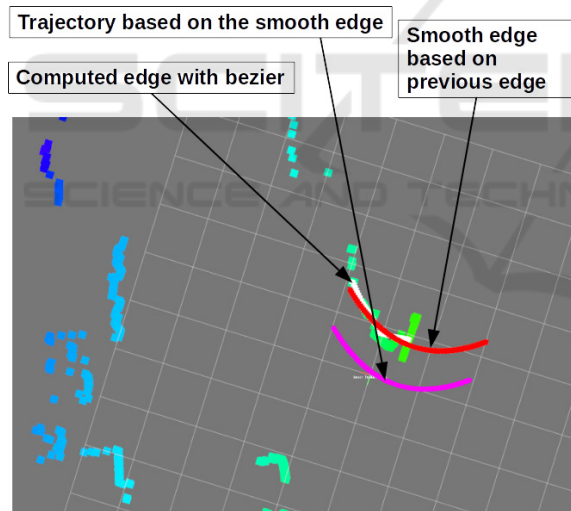


Figure 8: Trajectory generation during the structure following in indoor conditions between C and D.

One can see in Fig. 8 the laser impact points on the shelf legs in green, the points of interest generated in white and the computed trajectory in red, using a second order polynomial curve fitting. The objective is to follow the various structures with a desired lateral deviation y_d of 1m. The results related to the tracking error e_y during this first experiment are depicted in Fig. 9. In this figure, one can see that when the trajectory is achievable, the error converges and stays around 0, with an accuracy of few centimeters.

This is especially the case when the robot is fol-

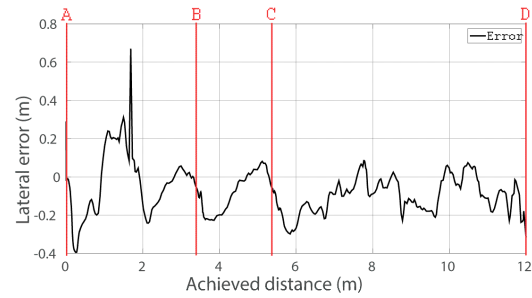


Figure 9: Result of the tracking error during the indoor experiment.

lowing the part between C and D, since the curvature stays quite low. In contrast, one can see important deviations:

- at curvilinear abscissa 1m, when the robot switches from the box on the right to the one on the left;
- around points B and C, when the robot has to follow high curvatures.

At these points, a discontinuity in the edge occurs. As a result, these errors are linked to the modification of the shape to be followed and can then be viewed as an initial error, canceled after the robot has moved.

Moreover, when the robot faces high curvatures, there is a risk of collisions and the desired orientation $\tilde{\theta}_d$ is bounded by $\tilde{\theta}_{col_right}$, as it is shown in Fig. 10. In this figure, the desired orientation $\tilde{\theta}_d$ is reported in magenta and compared with the actual one θ in blue. The minimal admissible orientation $\tilde{\theta}_{col_right}$ is reported in red (maximal in terms of absolute value). One can then see that at each large deviation (just after points B and C), when the robot has to achieve an almost 90° turn, the minimal value bounds the desired value to avoid collisions. As a result, the tracking error is not correctly regulated since the minimal value is imposed instead of the one required to reach the desired lateral deviation y_d . The same phenomenon can be observed around curvilinear abscissa 9m. Elsewhere, the minimal acceptable value stays far from the desired one and may reach 90°, which is the default value.

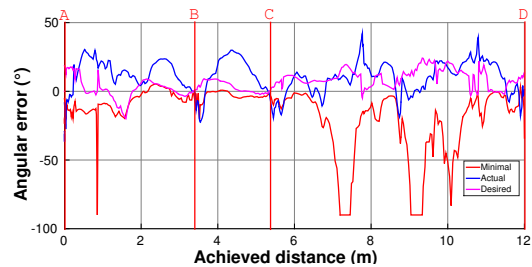


Figure 10: Desired, actual, and minimal orientations during the indoor experiment.

5.3 4WS Robot in Outdoor Conditions

The second experiment proposed in this paper consists in an outdoor structure following by a four-wheel-steering robot. Here, the objective is to follow a row of trees such as depicted in Fig. 6(b), with a desired distance of 1.5m and the robot parallel to this structure (i.e. $\tilde{\theta}_r = 0$). In these conditions, the structure is almost straight. As it can be seen in Fig. 11, the trajectory generated (in red) is indeed nearly considered as a straight line, even if the impact points of the laser (in yellow) are quite noisy.

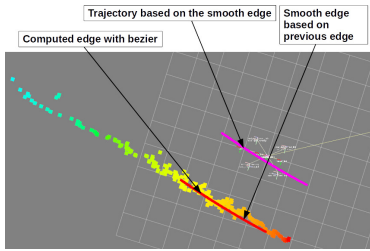


Figure 11: Trajectory generation during the structure following in outdoor conditions.

Thanks to the generation of the trajectory, the robot is able to follow accurately the row of trees, as illustrated by the tracking error shown in Fig. 12. One can see that after the initialization phase, the error converges to zero and remains then close to this value. One can also notice that the obtained accuracy is in the order of few centimetres.

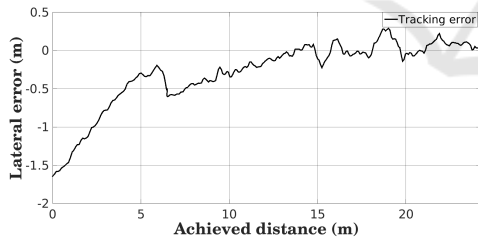


Figure 12: Result of the tracking error during the outdoor experiment.

This convergence is obtained thanks to the desired orientation control proposed in this paper. The desired orientation $\tilde{\theta}_d$ is illustrated in Fig.13 in magenta. The maximal admissible angle (the robot follows on the left), depicted in red in this figure, stays far from the desired orientation, and does not disturb in this case the accuracy of the tracking. One can nevertheless see that this maximal orientation logically decreases, as soon as the robot comes closer and closer from the actual structure. Since the desired distance has been set to 1.5m ($y_d = 1.5m$) and the half-track of the robot is equal to 0.6m, the robot rear left wheel could collide the trees if the lateral er-

ror reaches 0.9m. This can be illustrated at curvilinear 18m, where the maximal admissible angle is close to the actual one, as depicted in Fig. 13.

The desired orientation is compared to the orientation $\tilde{\theta}_2 = \tilde{\theta} + \delta^R$ which is the variable actually controlled for a 4WS robot (as detailed in section 3.3) and illustrated in black. Despite some disturbances, one can see a good correlation that allows to obtain the satisfactory lateral position regulation illustrated in Fig. 12.

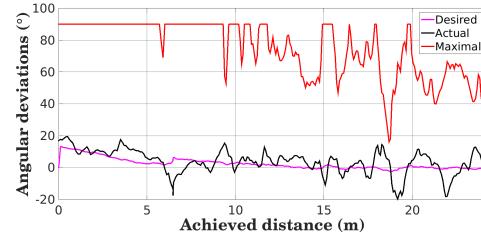


Figure 13: Desired, actual, and maximal orientations during the outdoor experiment.

It can also be verified that the rear steering law allows to keep the robot parallel to the structure, as desired (since $\tilde{\theta}_r = 0$). This can be particularly emphasized when focusing on the initialization phase of the tracking (before the settling distance of 6m has been reached). Fig. 14 compares the orientation $\tilde{\theta}_2$, in black, and the actual one $\tilde{\theta}$ in blue, from 0m to 6m. Since the desired orientation $\tilde{\theta}_d$ stays below 15° , the desired actual angle $\tilde{\theta}_r$ is null, as figured out by the relationship (24).

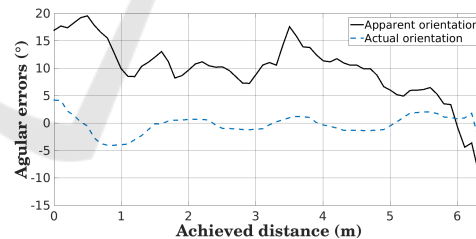


Figure 14: Comparison between $\tilde{\theta}_2$ and the actual orientation $\tilde{\theta}$.

Thanks to control laws (22), the actual orientation $\tilde{\theta}$, whose initial value is 5° converges and stays close to zero, while the rear steering angle permits to converge to a null tracking error. This point is particularly important when considering agricultural tasks.

6 CONCLUSION

In this paper, a generic control algorithm for tracking accurately a structure at a desired distance is proposed, based on an edge detection by a Lidar. It per-

mits to address in a common framework, several kinds of mobile robots, thanks to a backstepping approach. A desired orientation is first computed, allowing the robot to converge to the desired distance from the structure to be followed, whatever its configuration (skid-steering, car-like, or four-wheel-steering). This is achieved using the derivative with respect to curvilinear distance, in order to have a behaviour which is independent from the velocity. Beyond the convergence of the lateral error, this first step also permits to detect and avoid collisions, by considering the minimal and maximal admissible orientation, inside the motion control framework. Moreover, this desired orientation is also used to compute a speed limitation for skid-steering mobile robots, allowing to achieve harsh manoeuvres. The second step consists in the regulation of the orientation of the robot to the desired one computed in the first step. For skid-steering robots, this is achieved relying on a model with derivatives w.r.t. time, allowing them to rotate even with a null longitudinal speed in order to enhance the manoeuvrability. For four-wheel-steering mobile robots (and consequently car-like mobile robots), a strategy based on the curvilinear abscissa is proposed, adding two steps in the approach. The front steering angle is first controlled to impose that the orientation $\tilde{\theta}_2$ (robot orientation increased by the rear steering angle) converges to the desired one and next the rear steering angle regulates the actual robot orientation to increase the manoeuvrability or to ensure the parallelism of the robot with respect to the structure to be followed, depending on the situation. Such an approach permits to regulate independently the position and the orientation of the robot.

The effectiveness of the proposed algorithm has been investigated through full scale experiments, showing its robustness and efficiency in various conditions, with different kinds of structures to be followed (indoor furnitures and vegetations) and with several kinds of robots. In particular, this algorithm has been successfully tested on a 25-kg skid-steering robot and on a 520-kg four-wheel-steering robot, showing the generality of the proposed control law(s). This opens the way to achieve fully autonomous agricultural tasks, especially in orchard or vineyard, for spraying application. A new robot, able to carry out an automated sprayer is indeed under development to test such an approach in fully working conditions.

ACKNOWLEDGMENT

This work has been sponsored by the French National Research Agency under the grant number ANR-14-CE27-0004 attributed to Adap2E project (adap2e.irstea.fr). It has also been sponsored by the French government research program "Investissements d'Avenir" through the IDEX-ISITE initiative 16-IDEX-0001 (CAP 20-25), the IMobS3 Laboratory of Excellence (ANR-10-LABX-16-01) and the RobotEx Equipment of Excellence (ANR-10-EQPX-44). This research was also financed by the European Union through the Regional Competitiveness and Employment program -2014-2020- (ERDF – AURA region) and by the AURA region.

REFERENCES

- Astrand, B. and Baerveldt, A.-J. (2005). A vision based row-following system for agricultural field machinery. *Mechatronics*, 15(2):251 – 269.
- Bayar, G., Bergerman, M., Koku, A. B., and Konukseven, E. I. (2015). Localization and control of an autonomous orchard vehicle. *Computers and Electronics in Agriculture*, 115:118 – 128.
- Bergerman, M., Billingsley, J., Reid, J., and Van Henten, E. (2016). Robotics in Agriculture and Forestry. In *Springer Handbook of Robotics*, pages 1463–1492. Springer International Publishing.
- Blackmore, S. (2016). Towards robotic agriculture. In *SPIE Commercial+ Scientific Sensing and Imaging*, pages 986603–986603. International Society for Optics and Photonics.
- Cariou, C., Lenain, R., Thuilot, B., and Martinet, P. (2010). Autonomous maneuver of a farm vehicle with a trailed implement: motion planner and lateral-longitudinal controllers. In *IEEE International Conference on Robotics and Automation (ICRA)*, pages 3819–3824.
- Cherubini, A. and Chaumette, F. (2013). Visual navigation of a mobile robot with laser-based collision avoidance. *The International Journal of Robotics Research*, 32(2):189–205.
- D'Andréa-Novel, B., Campion, G., and Bastin, G. (1995). Control of nonholonomic wheeled mobile robots by state feedback linearization. *The International journal of robotics research*, 14(6):543–559.
- Deremetz, M., Lenain, R., Couvent, A., Cariou, C., and Thuilot, B. (2017). Path tracking of a four-wheel steering mobile robot: A robust off-road parallel steering strategy. In *European Conference on Mobile Robots (ECMR)*, pages 1–7.
- Lenain, R., Deremetz, M., Braconnier, J.-B., Thuilot, B., and Rousseau, V. (2017). Robust sideslip angles observer for accurate off-road path tracking control. *Advanced Robotics*, 31(9):453–467.
- Marmoiton, F. and Slade, M. (2016). Toward Smart Autonomous Cars. In *Intelligent Transportation Systems:*

From Good Practices to Standards, pages 84–109. CRC Press.

Samson, C., Morin, P., and Lenain, R. (2016). Modeling and control of wheeled mobile robots. In *Springer Handbook of Robotics*, pages 1235–1266. Springer.

Tourrette, T., Lenain, R., Rouveure, R., and Solatges, T. (2017). Tracking footprints for agricultural applications: a low cost lidar approach. In *IEEE/RSJ International Conference on Intelligent Robots and Systems: Agri-Food Robotics Workshop*.

